Original Article

Asian Pacific Journal of Tropical Biomedicine

apjtb.org

doi: 10.4103/2221-1691.380563

Impact Factor® 1.7

Characterization and antimicrobial, antioxidant, and anti-proliferative activities of green synthesized magnesium oxide nanoparticles with shoot extracts of *Plicosepalus curviflorus*

Reem Hamoud Alrashoudi[1], Manal Abudawood[1], Ayesha Mateen[1]✉, Hajera Tabassum[1], Noura Ibrahem Alghumlas[1], Sabiha Fatima[1], Basmah Almaarik[1], Farah Maqsood[2], Nawal M. Al Musayeib[3], Musarat Amina[3]

[1]*Clinical Laboratory Sciences Department, College of Applied Medical Sciences, King Saud University, Riyadh 12372, Saudi Arabia*

[2]*Department of Optometry and Vision Science, College of Applied Medical Science, King Saud University, Riyadh 11451, Saudi Arabia*

[3]*Department of Pharmacognosy, College of Pharmacy, King Saud University, Riyadh 11495, P.O. Box 22452, Saudi Arabia*

ABSTRACT

Objective: To synthesize magnesium oxide nanoparticles using ethanol extract of shoots of *Plicosepalus curviflorus* (PC-MgONPs) and evaluate the antimicrobial, antioxidant, and anti-proliferative activities of PC-MgONPs.

Methods: The green synthesized PC-MgONPs were characterized by ultraviolet-visible (UV), Fourier-transform infrared spectroscopy, zeta potential, energy dispersive X-ray, and scanning electron microscopy. Furthermore, we investigated total antioxidant capacity and antimicrobial and anti-proliferative activities using breast cancer cell lines (MDA-231).

Results: The UV spectrum of PC-MgONPs showed a sharp absorption peak at 300 nm. The presence of magnesium, oxygen, and sodium was confirmed by energy dispersive X-ray analysis. Scanning electron microscopy revealed PC-MgONPs as roughly spherical granular structures with sizes ranging from 20.0 to 76.4 nm. PC-MgONPs showed considerable antimicrobial activities against *Escherichia coli*, *Staphylococcus aureus*, methicillin-resistant *Staphylococcus aureus*, *Pseudomonas aeruginosa* and *Candida albicans* with zones of inhibition of 11-17 mm. In addition, total antioxidant capacity and anti-proliferative activity of PC-MgONPs against MDA-231 cells were dose-dependent.

Conclusions: The synthesized PC-MgONPs could be a potent antimicrobial, antioxidant and anti-cancer agent, which needs further investigation.

KEYWORDS: PC-MgONPs; *Plicosepalus curviflorus*; FTIR; Antimicrobial; Cell viability; Antioxidant

1. Introduction

Magnesium oxide nanoparticles (MgONPs) are interesting nanomaterials with excellent surface reactivity, promising biomedical applications, remarkable stability under harsh conditions, and less harmful effects, and can be employed as economical precursors[1]. These nanomaterials have shown potential biomedical features, including, antioxidant, antimicrobial, anticancer, anti-inflammatory, anti-diabetic, bone regeneration, and analgesic

Significance

Magnesium oxide nanoparticles (MgONPs) have emerged as attractive nanomaterials with diverse biomedical applications due to their distinctive physicochemical features, including biocompatibility, high stability, biodegradability, cationic capacity, and redox properties. The current study reports the synthesis of MgONPs using ethanol extract of *Plicosepalus curviflorus* shoot and MgONPs show antibacterial, antioxidant, and anti-proliferative activities.

✉To whom correspondence may be addressed. E-mail: amateen.c@ksu.edu.sa

How to cite this article: Alrashoudi RH, Abudawood M, Mateen A, Tabassum H, Alghumlas NI, Fatima S, et al. Characterization and antimicrobial, antioxidant, and anti-proliferative activities of green synthesized magnesium oxide nanoparticles with shoot extracts of *Plicosepalus curviflorus*. Asian Pac J Trop Biomed 2023; 13(7): 315-324.

Article history: Received 17 May 2023; Revision 1 June 2023; Accepted 28 June 2023; Available online 13 July 2023

effects[2-4]. MgONPs are utilized as ointments for the treatment of heart burns, wounds, and bone regeneration. These nanoparticles also exhibited excellent toxic properties against a wide range of human diseases that are resistant to many drugs[5]. Compared to other metal nanoparticles, MgONPs have many benefits, including non-toxicity, biocompatibility, cost-effectiveness, and stability, possessing important medical uses and potent antibacterial properties[6]. The Food and Drug Administration has determined that magnesium oxide (MgO) is generally recognized as safe for use in human food[7]. Moreover, recently, the Food and Drug Administration has authorized the use of magnesium sulphate injection in the treatment of preeclampsia in order to prevent seizures in patients[8].

Plicosepalus curviflorus (*P. curviflorus*) grows natively in Saudi Arabia, Yemen, East Africa, and Northeast Africa[9]. In Saudi Arabia, the entire plant has been used in traditional medicine to heal diabetes and in Yemen, the stem and heated twigs of this plant have been used in cancer treatment and as a poultice on the chest to cure pneumonia, respectively[10]. The flavane gallates, triterpenes, quercetin, catechin, and sterols found in the shoot extracts have antioxidant, hypoglycemic, antibacterial, cytotoxic, and anti-diabetic effects[11].

The aerial portions of *P. curviflorus* have been selected for green synthesis of MgONPs as the shoot part of the selected plant possesses active phenolic compounds (catechin, curviflorside, and curviflorin) with strong antibacterial and anti-proliferative activities, which we have isolated in our previous study[12]. Green synthesis of plant-based nanoparticles from metals, especially magnesium, and MgO, was used for numerous purposes[13,14]. The study aims to synthesize MgONPs using shoot extracts of *P. curviflorus* (PC-MgONPs) as the above-mentioned compounds are involved in the reduction, capping, and stabilization of formed nanoparticles as well as enhancement of biological properties of biosynthesized MgONPs. The antimicrobial, antioxidant, and anti-proliferative effects of MgONPs were also evaluated.

2. Materials and methods

2.1. Preparation of P. curviflorus ethanol extracts

The ethanol extract was prepared by macerating dried powder of *P. curviflorus* shoots (500 g) in ethanol (2 L × 3, each) for 8 h using a Soxhlet apparatus at room temperature. The solvent was chosen based on its solubility, and safety, and solvents with polarity values close to solute polarity perform better extraction. The resultant ethanol extract was filtered and subsequently liberated from the organic solvent by rotary evaporation at 50 ℃ under decreased pressure, yielding dark green ethanol extract (14.0 g).

2.2. Green synthesis of MgONPs using biomass of P. curviflorus

The green synthesis of PC-MgONPs was carried out by adding freshly prepared 1.0 mM magnesium nitrate (1.02 g of magnesium nitrate dissolved in 100 mL of distilled water) solution into 100 mL of *P. curviflorus* solution (5 g dissolved in 200 mL of ethanol) and stirred continuously at 600 rpm at 80 ℃ for 6 h with a magnetic stirrer (HJ-3 Thermostatic Magnetic Stirrer, Jiangsu, China). Afterward, 10 mL of NaOH (1.0 M) was poured dropwise into the reaction mixture to form a precipitate. The color change from green to dark brown was used to monitor the creation of nanoparticles. The reaction mixture was then centrifuged at 5 000 rpm for 15 min, the recovered precipitate was washed several times with ethanol to remove impurities, and dried PC-MgONPs (7.5 g) were calcined at 400 ℃ in a furnace. The mechanism of formation of PC-MgONPs was represented by the following equation:

$$Mg(NO_3)_2 \cdot 6H_2O + H_2O \xrightarrow{\text{Plant metabolites}} Mg(OH)_2 \quad (\text{Ⅰ})$$

$$Mg(OH)_2 \xrightarrow{400\,℃} MgO \quad (\text{Ⅱ})$$

2.3. Spectroscopic and microscopic characterization of PC-MgONPs

The formation of PC-MgONPs was confirmed by measuring the typical peak through a UV-Vis spectrophotometer at an absorption wavelength range of 200 to 800 nm (Shimadzu Corporation, Kyoto, Japan). FTIR analysis was performed to detect functional moieties and operated in a 400-4 000 cm^{-1} spectral range (Spectrometer-vector 22, Bruker, Germany). The crystalline structure of pre-synthesized PC-MgONPs was confirmed by X-ray diffraction (XRD) using Miniflex 600, X-ray diffractometer, Holland and it was operated at 40 kV with a current of 30 mA using CuKα radiation at 2θ angle ranging from 20 ℃ to 80 ℃. The stability and size distribution of the formed PC-MgONPs were assessed by zeta potential (ZP) and dynamic light scattering (DLS) using a particle size zeta potential analyzer based on laser light scattering (Zetasizer NS-3000, Malvern Analytical Ltd, Malvern, United Kingdom). The surface morphological features, including size, shape, and composition of PC-MgONPs, were monitored by scanning electron microscopy (SEM) equipped with energy-dispersive X-ray (EDX) spectroscopy using Zeiss SEM (Zeiss MultiSEM-505, Jena, Germany) with spectral images. Also, the elemental composition of the PC-MgONPs was estimated through EDX.

2.4. Preparation of stock solutions

The working stock solution was prepared by weighing 100 mg of *P. curviflorus* ethanol extracts and dissolved in dimethyl sulfoxide at a concentration of 100 mg/mL. PC-MgONPs was weighed and

dissolved in a solution containing sterile distilled water and nitric acid (4.8 mL water + 0.2 mL of nitric acid) to get the concentration of 10 mg/mL.The stock solution prepared were used to evaluate cell viability, antimicrobial and total antioxidant activity.

2.5. Microbial cultures

In the present study, five microbial strains were used to evaluate antimicrobial activity and minimum inhibitory concentration (MIC) of *P. curviflorus* ethanol extracts and PC-MgONPs. Three ATCC (American Type Culture Collection) microbial strains were used including *Escherichia coli* (*E. coli*, ATCC 25922), *Staphylococcus aureus* (*S. aureus*, ATCC 29213) and *Candida albicans* (*C. albicans*, ATCC 10231). Two clinical isolates [methicillin-resistant *S. aureus* (MRSA) and *Pseudomonas aeruginosa* (*P. aeruginosa*)] were used for the antimicrobial sensitivity.

2.6. Evaluation of antimicrobial activity

2.6.1. Agar well diffusion assay

The antimicrobial activity of PC-MgONPs was performed by agar well diffusion method. The bacterial cultures were grown in Muller Hinton broth (MHB) for 12-18 h and the turbidity of bacterial cultures was adjusted to a 0.5 McFarland standard (1×10^8 CFU/mL). One mL of bacterial culture (1×10^8 CFU/mL) was pipetted into the center of a sterile Muller Hinton agar (MHA) petri dish and spread on the plate using a spreader and wells were made into agar plates containing inoculums using a sterile cork borer (6 mm in diameter). Then, 100 µL of stock solution of the plant extract (100 mg/mL) and PC-MgONPs (10 mg/mL) were added to agar wells as test samples, and a disc of standard antibiotic (gentamycin) was used as a standard control.

The culture plates were incubated at 37℃ for 18-24 h. The zone of inhibition (including the diameter of the wells) was measured to detect antimicrobial activity[15].

2.6.2. MIC assay and IC_{50} calculation

The MIC of the plant extract (100 mg/mL) and PC-MgONPs (10 mg/mL) stock solution was determined by broth microdilution method, using sterile 96-well polystyrene cell culture plates. The microdilution plate was prepared by adding 100 µL MHB from well 2 to well 12. The first well contained 200 µL of the plant extract and PC-MgONPs and serial double dilution from wells 1 to 10 was performed by transferring 100 µL from each well. Finally, 10 µL of bacterial suspension was added to all the wells except well 12. Well 11 was kept as a positive control containing MHB and bacteria suspension, while well 12 was marked as a negative control containing only MHB. Next, the plates were incubated at 37℃ for 18-24 h. After incubation, a freshly prepared 3-(4,5-dimethylthiazol-2-yl)-2,5-diphenyltetrazolium bromide (MTT) reagent in sterile water at 0.5 mg/mL stock solution of volume 40 µL was added to each well and incubated at 37℃ for 30 min, and plates were measured at an absorbance of 600 nm in a microplate reader (SpectraMax plus 384). The experiment was done in triplicate[16,17].

The IC_{50} calculations were performed using the online QuestGraph™ IC_{50} Calculator online link (https://www.aatbio.com/tools/IC_{50}-calculator)[18].

2.7. Determination of total antioxidant capacity (TAC)

The *in vitro* antioxidant potential of PC-MgONPs was performed by TAC assay TAC using a total antioxidant capacity kit, MK-187, Sigma. Briefly, the test involves the reduction of Cu^{2+} ion to Cu^{+} by small molecules and proteins. The reduced Cu^{+} ion chelates with a colorimetric probe, giving a broad absorbance peak at 570 nm, which is proportional to TAC[19].

2.8. Determination of cell viability/proliferative activity

The cell viability of PC-MgONPs against a breast cancer cell line (MDA-231) was evaluated using the MTT assay. The cancer cells were grown in Dulbecco's Modified Eagle Medium supplemented with 1% antibiotic and 10% of fetal bovine serum solution in a humidified incubator with 5% CO_2 at 37℃. To measure cell inhibition, an MTT assay was performed. The cancer cells were seeded in 96-well plates at a density of 1×10^5 and incubated at 37℃ for 1 d. During the incubation time, cells were treated with PC-MgONPs (500, 250, 125, 62.5, 31.25, and 15.62 µg/mL) and *P. curviflorus* (5 000, 2 500, 1 250, 625, 312.5 and 156.25 µg/mL) for additional 24 h at 37℃. Then, 10 µL of MTT reagent solution was added to each well, and the plates were incubated at 37℃ for 4 h. With the addition of 100 µL of dimethyl sulfoxide, the purple-colored formazan crystals were dissolved. The absorbance was measured at 570 nm using a multiplate reader[20].

The cell inhibition percentage was calculated with the equation: Cell inhibition (%) = $100 - (OD_{test}/OD_{control} \times 100)$.

2.9. Statistical analysis

Statistical analyses were performed in triplicates using one-way ANOVA and data were presented as mean ± standard deviation. A *P*-value < 0.05 was considered significantly different. The GraphPad Prism Software 5th version for Windows, La Jolla, CA was used to perform statistical analysis.

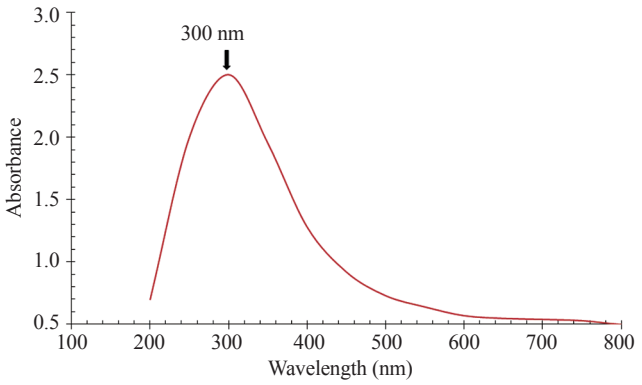

Figure 1. UV-Vis spectra of magnesium oxide nanoparticles using shoot extracts of *Plicosepalus curviflorus* (PC-MgONPs).

3. Results

3.1. UV–Vis spectral analysis

The formation of PC-MgONPs was confirmed by UV-Vis spectroscopy (wavelength range: 200-800 nm). A characteristic SPR absorbance peak was observed at 300 nm which verified the formation of PC-MgONPs (Figure 1).

3.2. FTIR spectroscopy

FTIR profile of *P. curviflorus* extract (Figure 2A) illustrated 13 peaks positions at 3 440.58, 2 995.75, 2 912.76, 2 194.79, 2 015.64, 1 660.45, 1 436.25, 1 406.56, 1 310.31, 1 018.46, 951.96, 697.67 and 667.22 cm^{-1}, whereas the PC-MgONPs reaction mixture elucidated 6 absorbance peaks sites at 3 292.18, 2 165.33, 2 150.41, 1 992.65, 1 633.88, and 1 338.33 cm^{-1} (Figure 2B). The absorbance peaks located between 3 000-3 600 cm^{-1} were allocated to the stretching vibrations of hydroxyl (-OH) amine (-NH) and (-CH) groups where -NH was characterized by a lower peak value than -OH.

According to FTIR data, the amide linkage of protein had a higher potential to bond with magnesium, resulting in the formation of a protein coating around MgONPs that prevents agglomeration and stabilizes the medium. In this study, the involvement of hydroxyl groups, amide group, and alkene functional groups in the bio-reduction process could be confirmed through the shift of the deformation vibration of O-H, -N-H, and –C=C groups positioned at 3 440.58 cm^{-1}, 2 194.79 cm^{-1}, and 1 660.45 cm^{-1} to 3 292.18 cm^{-1}, 2 165.33 cm^{-1}, and 1 633.88 cm^{-1}, respectively. Thus, it is reasonable to conjecture that hydroxyl, amine alkene, and alkyne functional groups present in the extract of *P. curviflorus* possibly perform both the capping and reduction process of nanoparticle formation.

XRD spectra analyzed the crystallinity and purity of biogenic-formed PC-MgONPs (Figure 3A), and the major XRD peaks of 2θ values were 36.8°, 42.4°, 61.8°, 74.9°, and 78.6°. The characteristic Bragg reflections were indexed location to (111), (200), (220), (311), and (222) lattice planes of face-centered cubic structure as compared with the standard reference (JCPDS file no.39-7746)[21] and these peaks confirmed the existence of MgONPs. The sharp diffraction pattern of pre-synthesized PC-MgONPs confirmed its high crystallinity and nano-size. Debye Scherrer's equation was applied to calculate the size of biogenic PC-MgONPs by using the width of the strongest peak (200) located at 42.4° (2θ value). The results revealed that the average crystallite size was 25 nm.

The average size distribution of the PC-MgONPs in the solution and the thickness of the capping or stabilizing compound enveloping metallic particles was determined by DLS. The results showed average particle size and polydispersity index (PDI) were 126.2 nm and 0.287 respectively (Figure 3B). The formed PC-MgONPs had a PDI of less than 0.7 demonstrating their high quality and reasonably well-defined dimensions with high monodispersity (PDI). The surface charge of pre-synthesized PC-MgONPs and the magnitude of charge were calculated by zeta potential and found to be 86.79 value.

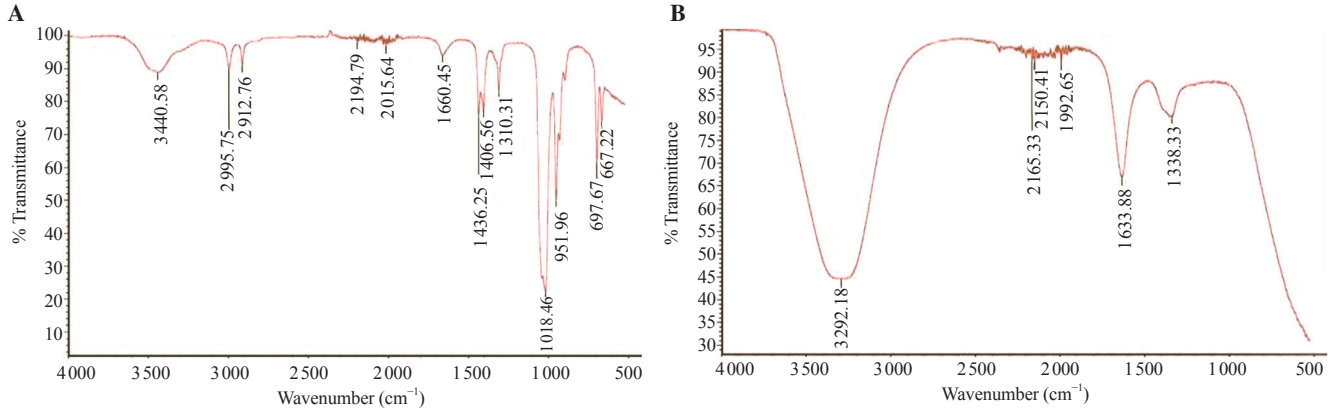

Figure 2. FTIR analysis of (A) *Plicosepalus curviflorus* and (B) PC-MgONPs.

3.3. Microscopic characterization of PC-MgONPs

SEM images of PC-MgONPs revealed that the particles had a spherical form and well-dispersed nanorods of PC-MgONPs that lacked any aggregation, with sizes ranging from 20.0 to 76.4 nm. In addition to producing a spherical shape that was well distributed and had a high ratio of surface area to volume, larger clusters were generated (Figure 4A). EDX spectra were used to analyze the elemental composition of PC-MgONPs (Figure 4B). The EDX graph revealed that the photo-mediated PC-MgONPs were exceedingly pure, displaying weight and atomic percentages of Mg (31.01%, 38.1%), O (55.1%, 51.3%), and Na (13.8%, 10.6%).

3.4. Antimicrobial activity, TAC, and anti-proliferative activity of PC-MgONPs

3.4.1. Antimicrobial activity

The antimicrobial activity of *P. curviflorus* extract and green synthesized PC-MgONPs was evaluated against *E. coli*, *S. aureus*, MRSA, *P. aeruginosa*, and *C. albicans*. PC-MgONPs were found to be effective against *E. coli* and *C. albicans* with a zone of inhibition of 17 and 16 mm, respectively (Figure 5 and Table 1).

In addition, *S. aureus* showed the least MIC value of 15.62 µg/mL and IC_{50} value of 7.17 µg/mL, whereas *E. coli* and *C. albicans* showed MICs of 31.25 and 62.50 µg/mL with IC_{50} values of 10.59 and 15.84 µg/mL, respectively (Table 2). *P. curviflorus* extracts showed the highest MIC values (1250 and 2500 µg/mL) against *S. aureus* and MRSA and showed a partial zone of inhibition.

Table 1. Diameter of zone of inhibition of PC and PC-MgONPs (mm).

Organisms	PC-MgONPs (10000 µg/mL)	PC (100000 µg/mL)	Gentamycin (10 µg/mL)
Escherichia coli	17	0	18
Staphylococcus aureus	11	16	19
MRSA	Partial	15	19
Pseudomonas aeruginosa	15	0	14
Candida albicans	16	0	NA

MRSA: methicillin-resistant *Staphylococcus aureus*; PC: *Plicosepalus curviflorus*; NA: not applicable.

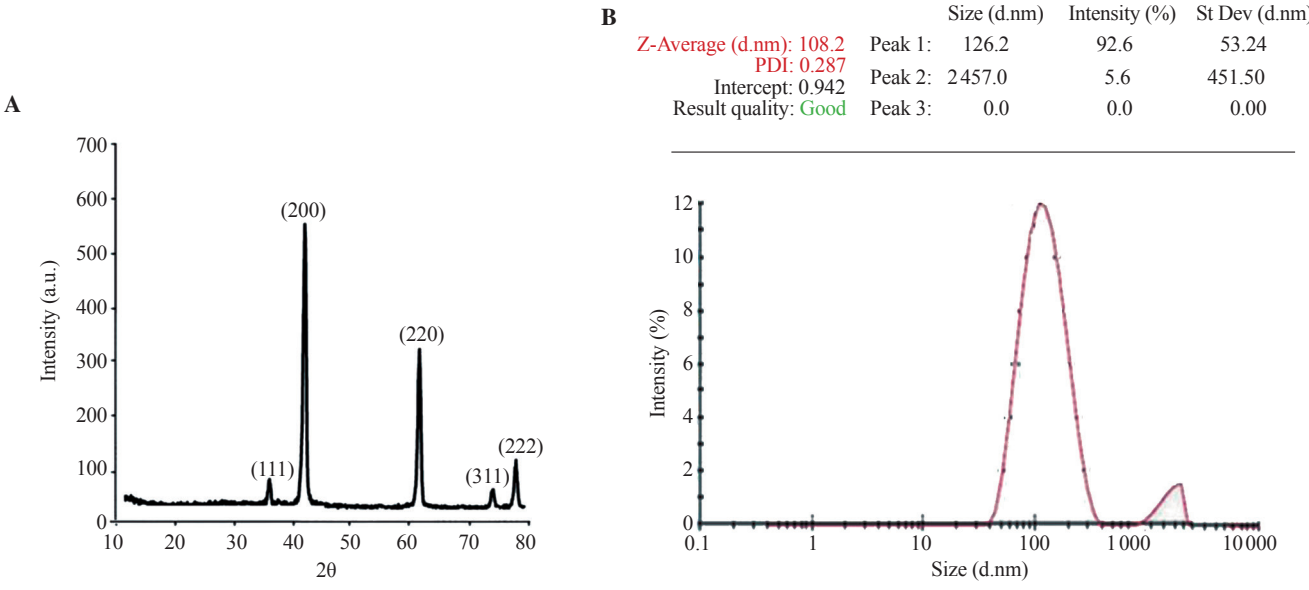

Figure 3. (A) X-ray diffraction spectrum and (B) size distribution analysis of PC-MgONPs.

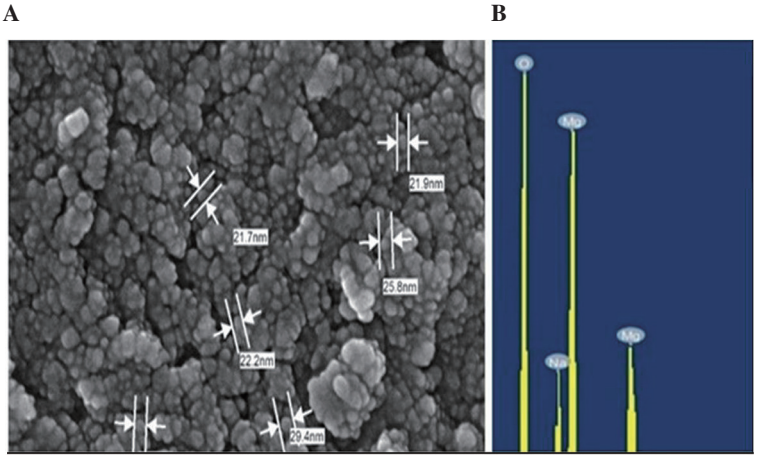

Figure 4. (A) Scanning electron microscopy and (B) energy dispersive X-ray analysis of biogenic PC-MgONPs. The arrow in the image represents the size of the particles (nm).

Table 2. Minimum inhibitory concentration (MIC) and IC_{50} values of PC-MgONPs and PC (μg/mL).

Organisms	PC-MgONPs		PC	
	MIC	IC_{50}	MIC	IC_{50}
Escherichia coli	31.25	10.59	NA	NA
Staphylococcus aureus	15.62	7.17	1250	NA
MRSA	62.50	28.66	2500	NA
Pseudomonas aeruginosa	125.00	43.24	NA	NA
Candida albicans	62.50	15.84	NA	NA

3.4.2. TAC

The results of TAC assay are illustrated in Figure 6A. The green synthesized PC-MgONPs displayed excellent antioxidant potential. As reflected in the figure, a dose-dependent pattern was observed in the antioxidant activity ranging from 0.042-0.360 nmol/mL. Moreover, 10 mg/mL of PC-MgONPs exhibited the highest TAC.

3.4.3. Anti-proliferative activity

PC-MgONPs and *P. curviflorus* extract showed a concentration-dependent decline in cell viability ($P < 0.05$). In addition, PC-MgONPs exhibited more significantly inhibitory effects against MDA-231 cell viability compared to *P. curviflorus* extract (Figure 6B-C).

4. Discussion

A biological approach for the synthesis of metal and metal oxide nanoparticles can be employed as an alternative to chemical and physical methods[22]. The benefits of biological synthesis, including its low cost, environmental friendliness, biocompatibility, scalability, and evasion of tough synthesis conditions like high temperature and pH, can be credited with this phenomenon[22]. Among biological entities, plants are recognized as promising entity for the biogenic synthesis of nanoparticles due to the presence of chemical components and high metal tolerances[23]. MgONPs are acknowledged by the FDA as a safe alternative to antibiotics with highly efficient antibacterial properties[7,24]. The ethanol extract of *P. curviflorus* shoots is a rich source of different types of bio-constituents including flavonoids, phenols, terpenes, steroids, proteins, and carbohydrates[12]. These phytocomponents might have contributed to the reduction, stabilization, and capping of produced PC-MgONPs, which plays a crucial role in the reduction of $Mg(NO_3)_2 \cdot 6H_2O$ to MgO-NPs. The hydroxyl and carbonyl groups of phytoconstituents serve as reducing and stabilizing substances[25]. The formation of biogenic PC-MgONPs initiates once the *P. curviflorus* extract is introduced into 1.0 mM $Mg(NO_3)_2$ solution. The gradual color change of $Mg(NO_3)_2$/*P. curviflorus* solution from dark

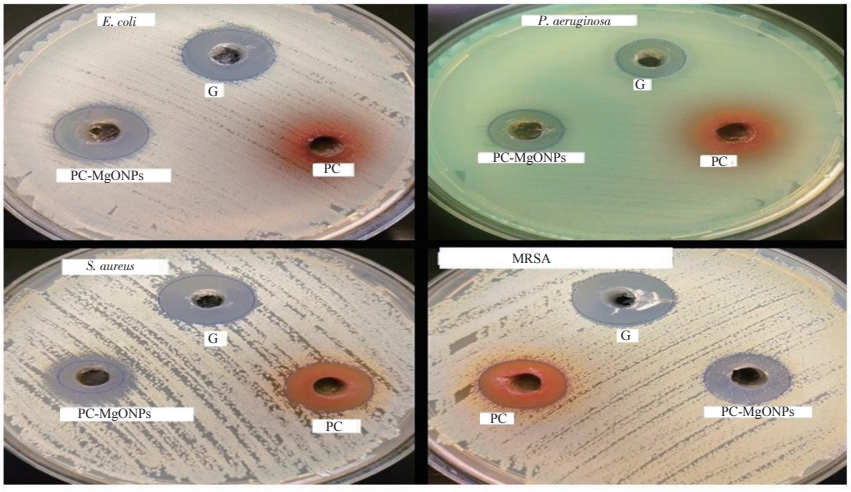

Figure 5. Antimicrobial effect of PC-MgONPs on the microbial strains by Agar well assay. G: gentamicin.

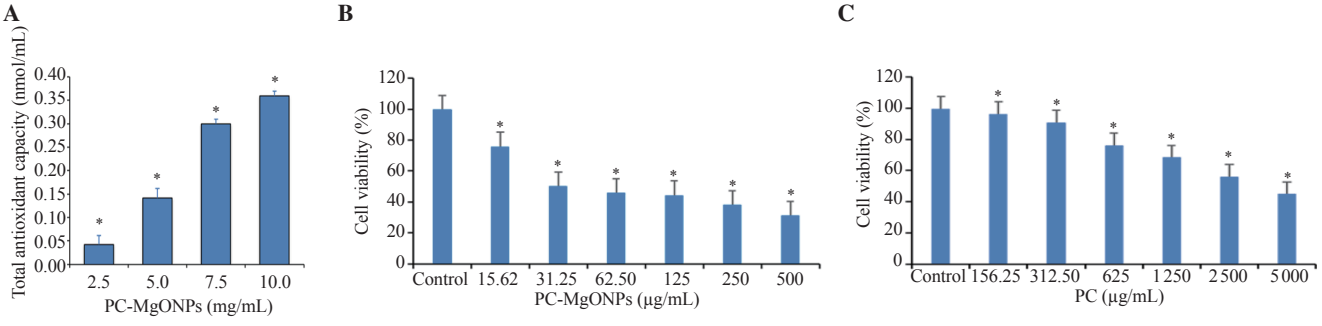

Figure 6. (A) Total antioxidant capacity and (B-C) anti-proliferative activity of PC-MgONPs and PC against breast cancer MDA-231 cells. $^{*}P<0.05$.

green to dark brown indicates the formation of PC-MgONPs. This color change can be attributed to the role of *P. curviflorus* metabolites in the reduction of NO_3^- to NO_2 followed by the reduction of Mg^{2+} to $Mg(OH)_2$ by liberated electrons. The maximum color intensity was attained due to the reduction of a large number of metal ions. The as-prepared $Mg(OH)_2$ was calcinated at 400 ℃ to form PC-MgONPs[26]. The formation of PC-MgONPs was further confirmed by different spectroscopic (UV-Vis, FTIR, XRD, ZI, DLS) and microscopic (SEM and EDX) techniques.

The UV-Vis spectroscopy analysis showed a characteristic SPR absorbance peak at 300 nm, which satisfies the standard MgO absorption pattern because all oxide nanomaterials have wide band gaps and a propensity for shorter wavelengths. The formation of PC-MgONPs was confirmed by UV-Vis spectroscopy (wavelength range: 200-800 nm)[27].

FTIR analysis was performed to identify the potential biomolecules that contributed to the bioreduction of magnesium oxide and stabilization of PC-MgONPs[28]. The presence of peaks between 2 100-2 250 cm^{-1} corresponds to alkyne (C≡C, C≡N) functional groups, and the peak appearance at 2 194.79 cm^{-1} in *P. curviflorus* extract and 2 165.33 cm^{-1} in PC-MgONPs indicates the presence of unsaturated hydrocarbons in the extract as well as in biogenic PC-MgONPs[29]. The appearance of prominent peaks at around 1 662-1 626 cm^{-1} is characteristic of the C=C stretching vibration type for disubstituted alkene. The peak shifting in the spectral profile of PC-MgONPs could be attributed to the interactions between those chemical functional groups and MgONPs[30]. It is reported in the literature that free amide groups in the protein molecules allow them to interact with MgONPs[31]. Our results exhibited broad distinctive spectral bands at 3 292.18-3 440.58 cm^{-1} are characteristics of the O-H stretching vibration type of hydroxyl functional moiety in polyphenols and N-H stretching vibration in primary and secondary amines (amino acids, proteins, and peptides) as well as hydrocarbons[32]. The results also indicate that some organic residues, such as hydroxyl and carboxyl groups, are present on the surface of the prepared PC-MgONPs.

The surface charge of pre-synthesized PC-MgONPs and the magnitude of charge were calculated by zeta potential and found to be 86.79 value, which illustrates the nanoparticle stability in dispersion by developing specific charge groups on their surface[33]. The result revealed that PC-MgONPs produced by *P. curviflorus* shoot extracts exhibited a charge on the surface of the PC-MgONPs, possibly due to free nitrate ions in the reaction mixture that provides repulsive force as electrostatic force stabilization[34]. Furthermore, no particle agglomeration was seen, as the formed PC-MgONPs were well dispersed. These results indicate that phytocomponents of the plant extract served not only as a reducing agent but also as a stabilizer, which protects the aggregation of MgONPs.

SEM analysis displayed spherical and well-dispersed nanorods of PC-MgONPs with sizes ranging from 20 to 76.4 nm[35]. The EDX graph revealed that the PC-MgONPs were exceedingly pure, displaying weight and atomic percentages of Mg (31.01%, 38.1%), O (55.1%, 51.3%), and Na (13.8%, 10.6%), which corresponds to the synthesis of MgO via ethanol extract of *P. curviflorus*[36].

PC-MgONPs were also found to be effective against *E. coli* and *C. albicans* with a zone of inhibition of 17 and 16 mm in contrast to other studies of MgONPs antibacterial activity which showed zero zones of inhibition against *E. coli* and *S. aureus*[37]. PC-MgONPs exhibited very effective effects in comparison with MgONPs[37]. Whereas, in our previous study, the biogenic green synthesis of MgONPs using *Saussurea costus* biomasses exhibited the highest MIC values for *E. coli* and *P. aeruginosa* in contrast to those of PC-MgONPs in our present research work[38].

Among the Gram-negative bacteria, *E. coli* was most sensitive to PC-MgONPs, because the Gram-negative bacteria are coated with lipopolysaccharide molecules, which have a negative charge and bind with positively charged MgO ions on the surface of PC-MgONPs, possibly leading to increased uptake of ions that damages the intracellular structures of Gram-negative bacteria[39].

As reported in the previous research, three compounds quercetin, catechin, and flavane gallate 2S, 3R-3,3′,4′,5,7-pentahydroxyflavane-5-*O*-gallate were isolated from the aerial parts of *P. curviflorus*[16], flavane gallate and catechin possess antimicrobial activity against various Gram-positive and Gram-negative pathogenic bacterial strains by binding to the lipid bilayer which damages bacterial membrane leading to inactivation and inhibition of intracellular and extracellular enzymes synthesis[40].

Numerous studies indicate that the antimicrobial activity of MgO is generally attributed to the production of reactive oxygen species (ROS), causing membrane breakdown and cellular content leakage. It has been shown that bacterial cells treated with MgONPs produce deep craters on their membrane surface, indicating that structural damage to the membrane leads to cellular content leakage. Whereas, our results showed PC-MgONPs had better antimicrobial activity than the plant extract which only showed antibacterial effects against *S. aureus* and MRSA. Nanoformulation of catechin and other active plant components had strong antibacterial activity, but in the present study, the plant extract exhibited less antimicrobial activity against the pathogenic microbial strains[41].

Although cellular oxidation is essential for cell proliferation, it also has some negative side effects due to the production of free radicals and ROS. Overproduction of these free radicals has severe consequences on the protective antioxidant system, which in turn causes cellular damage by oxidizing essential macromolecules, ultimately resulting in apoptosis/cell death. TAC analysis confirmed PC-MgONPs possess superior antioxidant capability, which may be

due to the capping effect of phytochemicals like flavonoids, which have several hydroxyl groups and phenolic functional groups on their surface, making synergistic effects. Our results both confirm and extend the work of previous researchers[42].

Moreover, curviflorin, curviflorside, flavonoids, and naphthalene were found in shoot parts of *P. curviflorus*[11], which possess strong antioxidant activity. Previous studies on the extracts of *P. curviflorus* and PC-MgONPs support our present findings. PC-MgONPs exhibited strong antioxidant activity which involves the redox potential of phytochemicals and the active compounds found in the *P. curviflorus* extract and the MgO antioxidant capability[43].

In our results, a decrease in cell viability of MDA-231 cells was observed as the concentration of PC-MgONPs and *P. curviflorus* extract increased, which may be attributed to the generation of ROS by PC-MgONPs, resulting in damages to mitochondrial membrane integrity and thus activation of the apoptotic pathway leading to cell death. The result was consistent with that found in a previous study in which *P. curviflorus* extract showed the expression of apoptosis-regulating genes including caspase-3, -8, -9, p53, Bax, and Bcl-2[29]. Contrary to what has been shown in the past, the toxicity of PC-MgONPs may be directly related to their size, with smaller-size PC-MgONPs being more hazardous because they generate more ROS that interact with cellular components and penetrate cell membranes, releasing Mg^{+} ions[36,44]. Among the phytochemicals, phenolic compounds such as catechin showed an anti-proliferative effect against lung cancer A549 cells by inhibiting cyclin E1 and p-AKT and induction of a potent cyclin kinase inhibitor. Moreover, epicatechin induces apoptosis in breast and prostate carcinomas[45].

To conclude, PC-MgONPs were successfully synthesized using *P. curviflorus* shoot extract. PC-MgONPs showed antimicrobial, antioxidant, and anti-proliferative properties. However, *in vivo* studies are needed to further verify their effects.

Conflict of interest statement

The authors declare that they have no conflict of interest.

Acknowledgments

The authors extend their appreciation to the Research Supporting Project number (RSPD2023R656), King Saud University, Riyadh, Saudi Arabia.

Funding

This work was funded by the Researchers Supporting Project Number (RSPD2023R656), King Saud University, Riyadh, Saudi Arabia.

Authors' contributions

RHA theorized and designed the research study, reviewed the literature, acquired data, and critically commented on the original draft of the manuscript. MA reviewed and edited the final draft of the manuscript. AM contributed to the conceptualization and design of the study, interpreted the results, and wrote the manuscript. HT designed the study and contributed to the discussion of the study. NIA managed data collection and analysis. SF interpreted the results. BA critically revised and edited the final version of the manuscript. FM critically commented on and edited the final version of the manuscript. NMA managed data collection. MA interpreted the results. All the authors have read and agreed with the published version of the manuscript.

References

[1] Thakur N, Ghosh J, Pandey SK, Pabbathi A, Das J. A comprehensive review of biosynthesis of magnesium oxide nanoparticles, and their antimicrobial, anticancer, and antioxidant activities as well as toxicity study. *Inorg Chem Commun* 2022; **146**. doi: 10.1016/j.inoche.2022.110156.

[2] Chen B, Lin Z, Saiding Q, Huang Y, Sun Y, Zhai X, et al. Enhancement of critical-sized bone defect regeneration by magnesium oxide-reinforced 3D scaffold with improved osteogenic and angiogenic properties. *J Mater Sci Technol* 2023; **135**: 186-198.

[3] Navya N, Ambika AV, Suresha BL. Synthesis, characterization, and anti-cancer potential study of Ag-MgO nanocomposite. *Inorg Chem Commun* 2022; **142**: 109671.

[4] Raissa U, Muhammad Abbas Qassem H, Ahmed M, Abdullateef Alzubaidi M, A Dawood F, Abdulamir Abdullah Y, et al. Investigating the effect of streptozotocin-induced diabetes on the ovarian tissue of NMRI mice following the injection of MgO and MgONPs. *J Nanostructures* 2023; **13**(1): 1-7.

[5] De Silva RT, Mantilaka M, Goh KL, Ratnayake SP, Amaratunga GAJ, de Silva KM. Magnesium oxide nanoparticles reinforced electrospun alginate-based nanofibrous scaffolds with improved physical properties. *Int J Biomater* 2017; **2017**. doi: 10.1155/2017/1391298.

[6] Akram MW, Fakhar-e-Alam M, Atif M, Butt AR, Asghar A, Jamil Y, et al. *In vitro* evaluation of the toxic effects of MgO nanostructure in Hela cell line. *Sci Rep* 2018; **8**(1): 4576.

[7] U.S. Food and Drug Administration. CFR—Code of federal regulations Title 21. [Online] Available from: https://www.accessdata.fda.gov/scripts/

cdrh/cfdocs/cfcfr/CFRSearch.cfm?fr=184.1431 [Accessed on 20th Dec 2022].

[8] Skylar Kenney AE. FDA approves magnesium sulfate injection from milla pharmaceuticals. *Pharm Times* 2022; **88**(1). [Online] Available from: https://www.pharmacytimes.com/view/fda-approves-magnesium-sulfate-injection-from-milla-pharmaceuticals [Accessed on 20th Dec 2022].

[9] Sher H, Alyemeni MN. Pharmaceutically important plants are used in the traditional system of Arab medicine for the treatment of livestock ailments in Saudi Arabia. *Afr J Biotechnol* 2011; **10**(45): 9153-9159.

[10]Al-Fatimi M, Wurster M, Schröder G, Lindequist U. Antioxidant, antimicrobial and cytotoxic activities of selected medicinal plants from Yemen. *J Ethnopharmacol* 2007; **111**(3): 657-666.

[11]Al Musayeib NM, Ibrahim SRM, Amina M, Al Hamoud GA, Mohamed GA. Curviflorside and curviflorin, new naphthalene glycoside, and flavanol from *Plicosepalus curviflorus*. *Z Für Naturforschung C* 2017; **72**(5-6): 197-201.

[12]Amina M, Al Musayeib NM, Alarfaj NA, El-Tohamy MF, Al-Hamoud GA, Alqenaei MK. The fluorescence detection of phenolic compounds in *Plicosepalus curviflorus* extract using biosynthesized ZnO nanoparticles and their biomedical potential. *Plants* 2022; **11**(3): 361.

[13]Huma T, Hakimi N, Younis M, Huma T, Ge Z, Feng J. MgO heterostructures: From synthesis to applications. *Nanomaterials* 2022; **12**(15): 2668.

[14]Silva AA, Sousa AMF, Furtado CR, Carvalho NM. Green magnesium oxide prepared by plant extracts: Synthesis, properties, and applications. *Mater Today Sustain* 2022; **20**. doi: 10.1016/j.mtsust.2022.100203.

[15]Balouiri M, Sadiki M, Ibnsouda SK. Methods for *in vitro* evaluating antimicrobial activity: A review. *J Pharm Anal* 2016; **6**(2): 71-79.

[16]Orfali R, Perveen S, Siddiqui NA, Alam P, Alhowiriny TA, Al-Taweel AM, et al. Pharmacological evaluation of secondary metabolites and their simultaneous determination in the arabian medicinal plant *Plicosepalus curviflorus* using HPTLC validated method. *J Anal Methods Chem* 2019; **2019**. doi: 10.1155/2019/7435909.

[17]National Committee for Clinical Laboratory Standards, Barry AL. *Methods for determining bactericidal activity of antimicrobial agents: Approved guideline*. Wayne, PA: National Committee for Clinical Laboratory Standards; 1999.

[18]AAT Bioquest, Inc. Quest Graph™ IC_{50} Calculator. AAT Bioquest. [Online] Available from: https://www.aatbio.com/tools/ic50-calculator [Accessed on 20th February 2022].

[19]Gupta S, Finelli R, Agarwal A, Henkel R. Total antioxidant capacity—Relevance, methods and clinical implications. *Andrologia* 2021; **53**(2). doi: 10.1111/and.13624.

[20]Kamiloglu S, Sari G, Ozdal T, Capanoglu E. Guidelines for cell viability assays. *Food Front* 2020; **1**(3): 332-349.

[21]Balakrishnan G, Velavan R, Batoo KM, Raslan EH. Microstructure, optical and photocatalytic properties of MgO nanoparticles. *Results Phys* 2020; **16**. doi: 10.1016/j.rinp.2020.103013.

[22]Jeevanandam J, Kiew SF, Boakye-Ansah S, Lau SY, Barhoum A, Danquah MK, et al. Green approaches for the synthesis of metal and metal oxide nanoparticles using microbial and plant extracts. *Nanoscale* 2022; **14**(7): 2534-2571.

[23]Ahmed SF, Mofijur M, Rafa N, Chowdhury AT, Chowdhury S, Nahrin M, et al. Green approaches in synthesising nanomaterials for environmental nanobioremediation: Technological advancements, applications, benefits and challenges. *Environ Res* 2022; **204**: 111967.

[24]Kumar H, Bhardwaj K, Kuča K, Kalia A, Nepovimova E, Verma R, et al. Flower-based green synthesis of metallic nanoparticles: Applications beyond fragrance. *Nanomaterials* 2020; **10**(4): 766.

[25]Madkour LH. Biogenic–biosynthesis metallic nanoparticles (MNPs) for pharmacological, biomedical and environmental nanobiotechnological applications. *Chron Pharm Sci J* 2018; **2**(1): 384-444.

[26]Adeyemi JO, Oriola AO, Onwudiwe DC, Oyedeji AO. Plant extracts mediated metal-based nanoparticles: Synthesis and biological applications. *Biomolecules* 2022; **12**(5): 627.

[27]Tanabe I, Tanaka YY, Watari K, Inami W, Kawata Y, Ozaki Y. Enhanced surface plasmon resonance wavelength shifts by molecular electronic absorption in far-and deep-ultraviolet regions. *Sci Rep* 2020; **10**(1): 9938.

[28]Ammulu MA, Vinay Viswanath K, Giduturi AK, Vemuri PK, Mangamuri U, Poda S. Phytoassisted synthesis of magnesium oxide nanoparticles from *Pterocarpus marsupium* rox. b heartwood extract and its biomedical applications. *J Genet Eng Biotechnol* 2021; **19**(1): 21.

[29]Eltamany EE, Goda MS, Nafie MS, Abu-Elsaoud AM, Hareeri RH, Aldurdunji MM, et al. Comparative assessment of the antioxidant and anticancer activities of *Plicosepalus acacia* and *Plicosepalus curviflorus*: Metabolomic profiling and *in silico* studies. *Antioxidants* 2022; **11**(7): 1249.

[30]Omdurman S. Synthesis and characterization of carbon nanotubes incorporated with MgO nanoparticles. *J Ovonic Res Vol* 2021; **17**(5): 429-435.

[31]Limo MJ, Sola-Rabada A, Boix E, Thota V, Westcott ZC, Puddu V, et al. Interactions between metal oxides and biomolecules: from fundamental understanding to applications. *Chem Rev* 2018; **118**(22): 11118-11193.

[32]Petit S, Decarreau A, Martin F, Buchet R. Refined relationship between the position of the fundamental OH stretching and the first overtones for clays. *Phys Chem Miner* 2004; **31**(9): 585-592.

[33]Negrescu AM, Killian MS, Raghu SN, Schmuki P, Mazare A, Cimpean A. Metal oxide nanoparticles: Review of synthesis, characterization and biological effects. *J Funct Biomater* 2022; **13**(4): 274.

[34]Pandiyaraj P, Gnanavelbabu A, Saravanan P. Prediction of stability and thermal conductivity of MgO nanofluids using CCRD statistical design analysis. *J Adv Chem* 2016; **12**(20): 5225-5236.

[35]Hassan SED, Fouda A, Saied E, Farag MM, Eid AM, Barghoth MG, et al. *Rhizopus oryzae*-mediated green synthesis of magnesium oxide nanoparticles (MgO-NPs): A promising tool for antimicrobial,

mosquitocidal action, and tanning effluent treatment. *J Fungi* 2021; **7**(5): 372.

[36]Fouda A, Eid AM, Abdel-Rahman MA, El-Belely EF, Awad MA, Hassan SED, et al. Enhanced antimicrobial, cytotoxicity, larvicidal, and repellence activities of brown algae, cystoseira crinita-mediated green synthesis of magnesium oxide nanoparticles. *Front Bioeng Biotechnol* 2022; **10**. doi: 10.3389/fbioe.2022.849921.

[37]Abinaya S, Kavitha HP. Magnesium oxide nanoparticles: Effective antilarvicidal and antibacterial agents. *ACS Omega* 2023; **8**(6): 5225.

[38]Amina M, Al Musayeib NM, Alarfaj NA, El-Tohamy MF, Oraby HF, Al Hamoud GA, et al. Biogenic green synthesis of MgO nanoparticles using *Saussurea costus* biomasses for a comprehensive detection of their antimicrobial, cytotoxicity against MCF-7 breast cancer cells and photocatalysis potentials. *PLoS One* 2020; **15**(8). doi: 10.1371/journal.pone.0237567.

[39]Slavin YN, Asnis J, Häfeli UO, Bach H. Metal nanoparticles: Understanding the mechanisms behind antibacterial activity. *J Nanobiotechnology* 2017; **15**(1): 65.

[40]Tsuchiya H. Membrane interactions of phytochemicals as their molecular mechanism applicable to the discovery of drug leads from plants. *Molecules* 2015; **20**(10): 18923-18966.

[41]Alavi M, Hamblin MR, Aghaie E, Mousavi SAR, Hajimolaali M. Antibacterial and antioxidant activity of catechin, gallic acid, and epigallocatechin-3-gallate: Focus on nanoformulations. *Cell Mol Biomed Rep* 2023; **3**(2): 62-72.

[42]Khan MA, Ali F, Faisal S, Rizwan M, Hussain Z, Zaman N, et al. Exploring the therapeutic potential of *Hibiscus rosa sinensis* synthesized cobalt oxide (Co_3O_4-NPs) and magnesium oxide nanoparticles (MgO-NPs). *Saudi J Biol Sci* 2021; **28**(9): 5157-5167.

[43]Amrulloh H, Fatiqin A, Simanjuntak W, Afriyani H, Annissa A. Antioxidant and antibacterial activities of magnesium oxide nanoparticles prepared using aqueous extract of *Moringa oleifera* bark as green agents. *J Multidiscip Appl Nat Sci* 2021. doi: 10.47352/jmans.v1i1.9.

[44]Tabrez S, Khan AU, Hoque M, Suhail M, Khan MI, Zughaibi TA. Investigating the anticancer efficacy of biogenic synthesized MgONPs: An *in vitro* analysis. *Front Chem* 2022; **10**. doi: 10.3389/fchem.2022.970193.

[45]Thomas P, Dong J. (-)-Epicatechin acts as a potent agonist of the membrane androgen receptor, ZIP9 (SLC39A9), to promote apoptosis of breast and prostate cancer cells. *J Steroid Biochem Mol Biol* 2021; **211**. doi: 10.1016/j.jsbmb.2021.105906.

Publisher's note